PROCESSES DEVELOPMENT FOR HIGH TEMPERATURE SOLAR THERMAL KALINA POWER STATION

by

N. Shankar GANESH[a] and Tangellapalli SRINIVAS[b*]

[a] Department of Mechanical Engineering, Kingston Engineering College, Vellore, Tamil Nadu, India
[b] CO_2 Research and Green Technologies Centre, School of Mechanical and Building Sciences, Vellore Institute of Technology University, Vellore, Tamil Nadu, India

Original scientific paper
DOI: 10.2298/TSCI120623020G

Kalina cycle system operates at a heat source temperature up to 600 ºC with an improved heat recovery. The current work focuses on thermodynamic processes development and assessment of a Kalina cycle system configuration to augment the power from a heat recovery of solar thermal collectors operating from 250 ºC to 600 ºC. There are three pressure levels in current cycle i. e. high pressure, intermediate pressure, and low pressure. The superheated vapor expands from high pressure to low pressure and the separator is located at intermediate pressure. The current work develops a new methodology for thermodynamic evaluation with more flexibility compared to the reported method in literature. Separator inlet condition (temperature and concentration), turbine inlet condition (pressure, temperature and concentration) and solar radiation have been identified as key parameters for the plant evaluation. The performance is improving with an increase in separator temperature, turbine inlet pressure, source temperature and solar radiation. But it is decreasing with an increase in separator and turbine inlet concentrations. The cycle efficiency, plant efficiency and specific power have been found as 23.5%, 7.5%, and 675 kW at 0.3 separator concentration and 0.5 turbine concentration.

Key words: *energy, efficiency, heat recovery, high temperature, Kalina, vapor absorption*

Introduction

Father of thermodynamics, Sadi Carnot said that "don't do any experimentation on power plant cycles unless theoretical analysis". Kalina cycle is a thermodynamic cycle, produces power utilizing binary mixture as working component. A well-known Kalina cycle according to Ibrahim and Klein [1] produces more power at a very high thermal capacitance ratio. In Rankine cycle more than half of the heat transfer occurs during the boiling process which is considered as constant temperature boiling process. In organic Rankine cycle (ORC) utilizing isopentene as working fluid, isopentene boils at a constant temperature under a given pressure. In ORC the theoretical efficiency and cost/production ratio are less. Kalina cycle has got large improvement in thermal efficiency, large reduction in cost, no combustion system, equivalent or lower capital costs, no major modifications to equipment used in conventional power plants, greater flexibility in operation, and no vacuum maintenance requirements. The invention was started in 1988 and the first construction started at 1990 in Canoga Park, Cal., USA [2]. First geothermal power station was started in 2000 at Husavik, Iceland [3].

* Corresponding author; e-mail: srinivastpalli@yahoo.co.in

In current work, the operational conditions for a Kalina cycle system have been developed with heat recovery at high temperature range (250-600 ºC). The plant under this study can be operated by a waste heat, solar concentrating collectors, diesel engine exhaust, gas turbine exhaust or cement/steel plant waste heat, *etc*. Heat is added in a combined boiling and separation process at a variable temperature. Heat is rejected in a combined condensation and absorption process as well at a variable temperature. Ammonia has a molar mass of 17 and steam has the molar mass of 18. Therefore steam turbines can be used with minor modifications in place of mixture turbine. The mixture properties are more complex, usually three independent properties are needed for the calculation of thermodynamic properties of mixtures. Therefore the cycle is more flexible and to be closely optimized at the energy source (*i. e*., solar, geothermal, exhaust of IC engines and gas turbines, *etc*.). Heppenstall [4] identified Kalina as a bottoming cycle and showed better performance compared to steam bottoming cycle. Thorin *et al*. [5] developed correlations for thermodynamic properties (temperature, pressure, volume, enthalpy, and entropy) of ammonia-water mixture which play an important role in calculating the performance of the power cycle. In Kalina cycle, the ratio of exergy loss with the net generated power was less compared with the Rankine cycle as per the Srinophakun *et al*. [6]. A comparison between Kalina cycle and ORC were made by Dippio [7] and concluded that among the binary plants, Kalina cycle generates 30% to 50% more power for a given heat source. Borgert and Velasquez [8] developed a Kalina cycle as a bottoming cycle for a co-generation plant by reducing the exhaust gas temperature from 427 K to 350 K. Mirolli [9] concluded that the distillation condensation subsystem technology is a key component for the high efficiency of a Kalina cycle plant for waste heat recovery power plant applications. Minea [10] stated that the Kalina cycle may produce power in the future especially with industrial waste heat and biomass. Wall and Ishida [11], Srinophakun *et al*. [6] and Wang *et al*. [12] solved the Kalina power cycle at high temperature heat recovery. The current work develops the new and simplified methodology compared to the reported solutions.

The main objective of the present work is to develop the best operational conditions to run the plant at high efficiency levels. The work also formulates the plant without iteration of configuration for parametric variations. Marston [13] carried out a parametric analysis for a Kalina power cycle with gas turbine exhaust's heat recovery and iteration has been carried out to the cycle loop with the initial assumption of separator inlet concentration. With this iteration, the separator inlet concentration becomes dependent and calculated after getting the consistency of the iteration. Similarly, Nag and Gupta [14] also solved the iteration with the initial assumption of vapor fraction and got the separator inlet concentration. These solutions have no flexibility on selection of separator inlet concentration or vapor fraction. The current new methodology allows selecting the separator inlet concentration without cycle iteration. So, present work develops more flexible solution compared to the published method.

Thermodynamic analysis of Kalina cycle

Following are the assumptions used in the assessment and analysis of plant. Atmospheric condition is taken as 1.01325 bar and 25 ºC. Hot source temperature is 500 ºC. High pressure (HP) is 100 bar. Terminal temperature difference (TTD) at heat recovery vapor generator (boiler) inlet with respect to the collector's hot fluid is taken at 10 ºC. Pinch point (PP) in boiler is 5 ºC. Approach point (AP) in the boiler is 10 ºC. The isentropic efficiency of solution pump and mixture turbine is considered as 75%. The mechanical efficiency of the solution pump ($\eta_{m,p}$) and mixture turbine ($\eta_{m,t}$) is taken at 96%. Electrical generator efficiency

(η_{ge}) is taken as 98%. The condensate leaving the condenser and absorber is assumed as saturated liquid. Pressure drop and heat losses in pipe lines are neglected.

The Kalina cycle considered in this work is suitable for high temperature heat recovery and shown in fig. 1. The working fluid, ammonia-water mixture is vaporized and superheated in heat recovery vapor generator (HRVG) before expansion in turbine. The superheated vapor (13) is expanded in the turbine (14) to transform its energy into useful form. The generated spent stream is then cooled in a HE_2 (15) and diluted with a weak solution (4) from throttle valve. A stream with a high concentration of ammonia, at the turbine outlet stream, cannot be condensed by cooling water of a normal temperature, since the high concentration of ammonia would result in a very low condensation temperature at the pressure level in the condenser. Therefore, the mixture concentration after dilution rises to condensing temperature and condensed in the absorber.

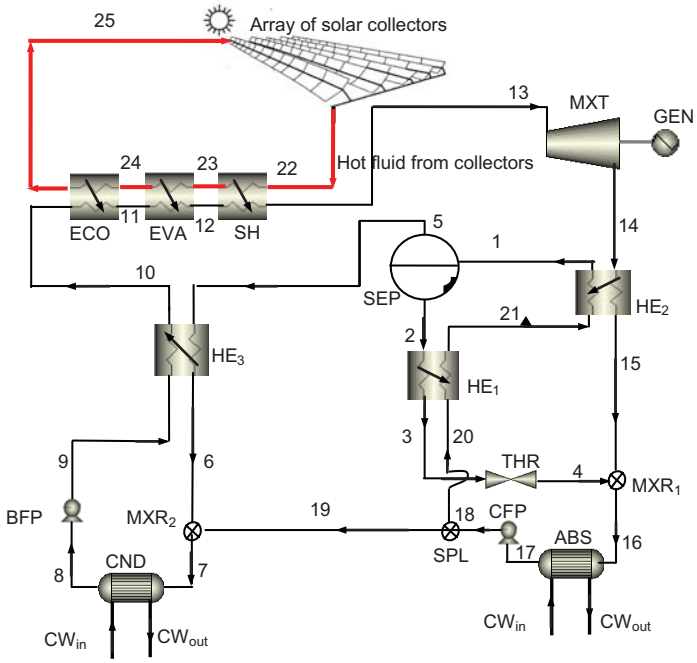

Figure 1. Schematic flow diagram of the Kalina cycle suitable to high temperature heat recovery
ABS – absorber; BFP – boiler feed pump; CFP – condensate feed pump; CND – condenser; CW_{in} – cooling water in; CW_{out} – cooling water out; ECO – economizer; EVA – evaporator; GEN – generator; HE – heat exchanger; HRVG – heat recovery vapor generator; MXR – mixer; MXT – mixture turbine; SEP – separator; SH – superheater; SPL – splitter; THR – throttling

The condensate pump increases condensate (18) pressure and passed through a splitter resulting in two streams. One of the two streams (20) is passed through the HE_1 and HE_2 recovering heat and admitted in the separator. The other stream (19) is mixed with the ammonia-rich vapor (6) from the separator to restore the working mixture concentration. From the separator, the stream (1) is separated to enriched vapor (5) and lean liquid (2). The ammonia lean liquid gives up heat in the HE_1, then throttled (4) and absorbs the working mixture stream (15) from the HE_2 before condensation in the low-pressure condenser. The other stream is condensed in the condenser (8), pressurized in a boiler feed pump (9) and sent into the boiler via HE_3. The economizer, evaporator, and super heater sections of HRVG supplies super heater vapor to the vapor turbine. The real focus of any power cycle is to increase the cycle efficiency by reducing the losses. Reduction in losses results an increased actual work.

The Kalina cycle has been solved at one kg mixture at the turbine inlet. The properties and mass flow rates around the loops are calculated by mass, concentration and energy balance equations. In the separator, liquid and vapor mixtures are separated. The absorber exit

temperature, T_{17} is a bubble point temperature at the intermediate pressure (IP). Figure 2 represents (a) enthalpy-concentration and (b) temperature-entropy diagram for a Kalina cycle in a solar thermal power plant operating under the conditions of P_{13} = 100 bar, T_{13} = 490 °C, x_{13} = 0.75, and T_1 = 80 °C. These two diagrams are plotted with reference to fig. 1. From fig. 2(a), it is observed that the cycle is operating under four concentrations *i. e.* 0.4, 0.59, 0.75, and 0.97. The lines 4-16-15 and 19-7-6 show the mixing processes, respectively, at MXR_1 and MXR_2. The line 2-1-5 shows about the separation process. The temperature-entropy plot, fig. 2(b), show that the condensation (16-17) and evaporation processes (11-12) transfers heat at variable temperature and reveals the benefit of binary mixture compared to single component. The separated liquid mass and vapor mass from mixture (1) are indicated at points 2 and 5, respectively.

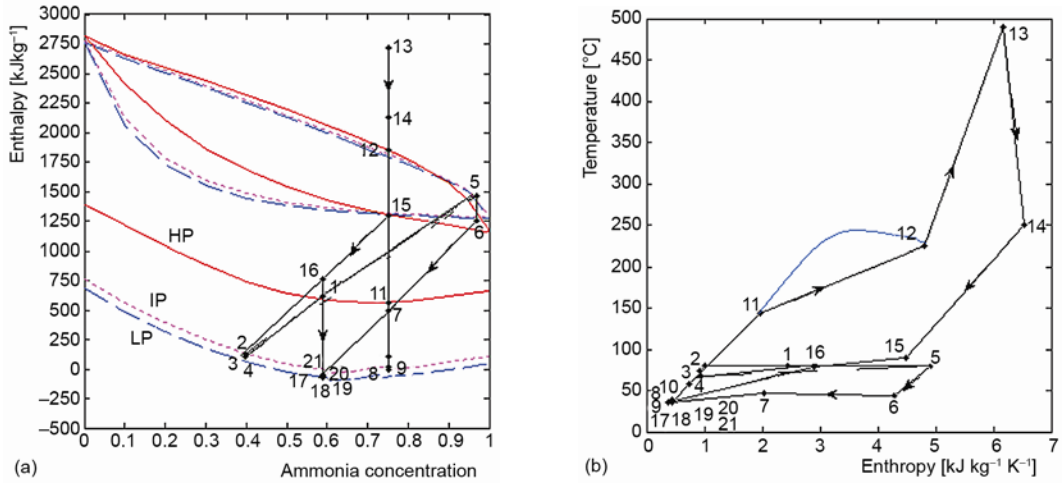

Figure 2. Temperature-entropy diagram for Kalina cycle with reference to fig. 1
(for color image see journal web-site)

Table 1 shows the properties of the working fluid (1-21) and hot fluid (22-25) at the state points, defined in fig. 1. The results are plotted at the separator temperature of 80 ºC, 1 kg/s of working fluid at turbine inlet and turbine concentration of 0.75. It results 490 ºC hot fluid inlet temperature and 0.59 of separator inlet concentration. A unit mass of working fluid in the power circuit demands 1.46 units of hot fluid at the above said conditions. Using mass and energy balance equations, eqs. (1) to (10), the unknown cycle properties have been obtained.

Let mass flow rate at the turbine inlet, m_{13} = 1 kg/s.

The intermediate pressure (IP) has been calculated from temperature and concentration at state 8. The liquid concentration (x_2) and vapor concentration (x_5) can be determined at separator pressure (IP) and its temperature. These three concentrations results vapor fraction (mass ratio vapor to total mixture). At separator, out of one kg/s of mixture, F [kgs^{-1}] is the vapor portion and $(1 - F)$ [kgs^{-1}] is the liquid portion to be separated. After applying lever rule for separation process:

$$F = \frac{m_5}{m_1} = \frac{x_1 - x_2}{x_5 - x_2}, \quad m_6 = m_5 = F\, m_1, \quad m_4 = m_2 = (1 - F)\, m_1 \tag{1}$$

Table 1. Material flow details of solar thermal power plant with reference to fig. 1

State	Pressure [bar]	Temperature [°C]	Ammonia concentration	Flow rate [kg s^{-1}]	Specific enthalpy [kJ kg^{-1}]	Specific entropy [kJ kg^{-1} K^{-1}]	Dryness fraction
1	9.66	80.00	0.59	1.25	619.98	2.43	0.363
2	9.66	80.00	0.40	0.83	129.35	1.00	0.000
3	9.66	74.51	0.40	0.83	104.42	0.93	0.000
4	6.37	66.95	0.40	0.83	105.10	0.93	0.043
5	9.66	80.00	0.97	0.42	1465.86	4.91	1.000
6	9.66	44.29	0.97	0.42	1248.71	4.27	0.928
7	9.66	46.68	0.75	1.00	491.11	2.03	0.368
8	9.66	35.00	0.75	1.00	–6.22	0.44	0.000
9	100.00	37.99	0.75	1.00	13.22	0.46	0.000
10	100.00	57.81	0.75	1.00	106.47	0.75	0.000
11	100.00	143.36	0.75	1.00	563.64	1.97	0.000
12	100.00	224.84	0.75	1.00	1849.68	4.80	1.000
13	100.00	490.00	0.75	1.00	2713.22	6.16	1.000
14	6.37	249.69	0.75	1.00	2122.56	6.53	1.000
15	6.37	90.20	0.75	1.00	1294.69	4.49	0.787
16	6.37	78.06	0.59	1.83	755.72	2.89	0.450
17	6.37	35.00	0.59	1.83	–71.46	0.37	0.000
18	9.66	36.13	0.59	1.83	–66.02	0.39	0.000
19	9.66	36.13	0.59	0.58	–66.02	0.39	0.000
20	9.66	36.13	0.59	1.25	–66.02	0.39	0.000
21	9.66	39.50	0.59	1.25	–50.60	0.43	0.000
22	–	500.00	–	1.46	1985.50	–	–
23	–	358.74	–	1.46	1395.02	–	–
24	–	148.36	–	1.46	515.65	–	–
25	–	73.57	–	1.46	203.04	–	–

At MXR_1:

$$m_4 + m_{15} = m_{16} \quad \text{and} \quad m_4 x_4 + m_{15} x_{15} = m_{16} x_{16} \tag{2}$$

Figure 3 simplifies the complex nature of Kalina cycle configuration into simple loops to solve the unknown mass at unit mass of turbine flow rate. The concentration at 1 and 13 are fixed and the properties at other points (2, 5, 17 and 19) are calculated.

Using expressions in eq. (2) we obtain:

$$\frac{m_4}{m_{15}} = \frac{x_{15} - x_{16}}{x_{16} - x_4}, \quad \text{or simplified} \quad m_2 = \frac{x_{13} - x_1}{x_1 - x_2} m_{13}, \tag{3}$$

At MXR_2 is:

$$m_6 + m_{19} = m_7,$$
$$m_6 x_6 + m_{19} x_{19} = m_7 x_7 \quad (4)$$

and

$$\frac{m_5}{m_{19}} = \frac{x_7 - x_{19}}{x_5 - x_7} = \frac{x_{13} - x_1}{x_5 - x_{13}} \quad (5)$$

To find m_1, at the separator, we use ratio:

$$\frac{m_1}{m_2} = \frac{x_5 - x_2}{x_5 - x_1} \quad (6)$$

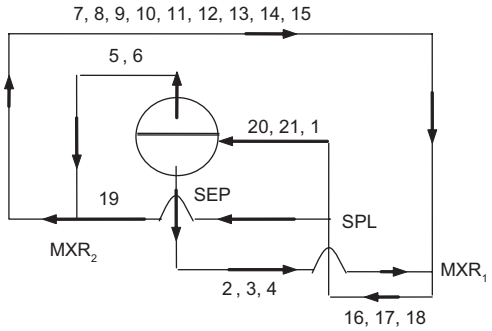

Figure 3. Looping of plant fluid flows for mass balance
MXR – mixer, SEP – separator, SPL – splitter

Substituting m_2 from eq. (3) and from eq. (1):

$$m_1 = \frac{x_5 - x_2}{x_5 - x_1}\frac{x_{13} - x_1}{x_1 - x_2} m_{13}, \quad m_1 = \frac{x_{13} - x_1}{F(x_5 - x_1)} m_{13} \quad (7)$$

To find m_{19} at the splitter, from MXR_2, we use ratio:

$$m_{19} = \frac{x_5 - x_{13}}{x_{13} - x_1} m_5 = \frac{x_5 - x_{13}}{x_{13} - x_1} m_1 F \quad (8)$$

substituting m_1 from eq. (17):

$$m_{19} = \frac{x_5 - x_{13}}{x_{13} - x_1}\frac{x_{13} - x_1}{F(x_5 - x_1)} F m_{13}, \quad m_{19} = \frac{x_5 - x_{13}}{x_5 - x_1} m_{13} \quad (9)$$

From eq. (7) and eq. (9), m_1 and m_{19} can be determined from x_1 at fixed mass, m_{13} and concentration, x_{13} as others are function of x_1. At MXR_1 dilution of vapor takes place with addition of m_4. Therefore x_1 should be less than x_{13}. The concentration difference (turbine concentration – separator inlet) has been varied from 4% to 20% in steps of 4% for parametric study. Based on this concentration difference, x_1 can be determined.

Hot fluid exit temperature from the collectors:

$$T_{13} = T_{22} - TTD_{SH} \quad (10)$$

Low pressure (LP) is function of temperature and concentration [$P_{17} = f(T_{17}, x_{17})$], so it is determined from the condenser temperature and vapor concentration.

The energy interactions in the plant components are:

– Mixture turbine output

$$w_t = m_{13}\,(h_{13} - h_{14})\eta_{m,t}\,\eta_{ge} \quad (11)$$

– Work input to pump

$$w_p = \frac{m_{18}(h_{18} - h_{17}) + m_9(h_9 - h_8)}{\eta_{m,p}} \quad (12)$$

– Net output from Kalina cycle

$$w_{\text{net}} = w_{\text{t}} - w_{\text{p}} \tag{13}$$

– Heat supply in boiler equations

$$q_{s1} = m_{13}(h_{13} - h_{12}), \quad q_{s2} = m_{12}(h_{12} - h_{11}), \quad q_{s3} = m_{11}(h_{11} - h_{10}) \tag{14}$$

– Kalina cycle energy efficiency

$$\eta_{\text{KC}} = \frac{w_{\text{net}}}{q_{s1} + q_{s2} + q_{s3}} \cdot 100 \tag{15}$$

The solar collector area and cost evaluation details, reported in the literature by the authors have been considered for the high temperature heat recovery Kalina power system [15].

Solar plant energy efficiency:

$$\eta_1 = \frac{w_{\text{net}}}{I_g A_{c\ \text{tot}}} \times 100 \tag{16}$$

Results and discussion

The performance of high temperature solar thermal power plant has been investigated parametrically under variable operational conditions. The influences of the key parameters *i. e.* separator concentration, separator temperature, turbine inlet condition (pressure, temperature and concentration) and solar radiation have been examined on the plant configuration. The parametric study has been conducted aiming at the maximization of the efficiencies and specific work.

Figure 4(a) shows the effect of concentration difference (4-20%) and separator temperature (60-100 ºC) on separator vapor fraction and LP. Turbine concentration has been selected as 0.75 because, it allows more variation in separator concentration and it is maintained below turbine concentration. The concentration difference is the difference in concentrations of turbine and separator inlet. From the difference, the separator inlet concentration can be obtained which gives the vapor fraction after finding the IP. The maximum possible concentration difference is found as 0.2 and 100 ºC of separator temperature. LP is changed from 5.5–9 bar and vapor fraction from 8-65% with the variations in separator concentration (by difference) and temperature. The vapor fraction decreased with increase in concentration difference (decrease in separator concentration) and increased with an increase in temperature. A raise in separator temperature decreases liquid and vapor concentrations with a rise in dew point temperature. The LP is evaluated at concentration and temperature at absorber exit. The absorber exit concentration is equal to the separator inlet concentration. Since there is no change in separator inlet concentration and absorber outlet temperature, the LP is constant irrespective of changes in separator temperature. The LP is decreasing with an increase in concentration difference (*i. e.* decrease in separator inlet concentration). The decrease in concentration also decreases vapor portion in separator. At concentration difference of 20% (turbine concentration of 75% and separator concentration of 55%), LP minimizes to 5.5 bar and results 8% of vapor fraction.

Figures 4(b) and (c) show the variation in solar plant thermal efficiency, cycle efficiency, and specific power with the effect of separator concentration and temperature. Under specified limits of operating conditions, the plant results 5.8-7.2% of solar plant efficiency,

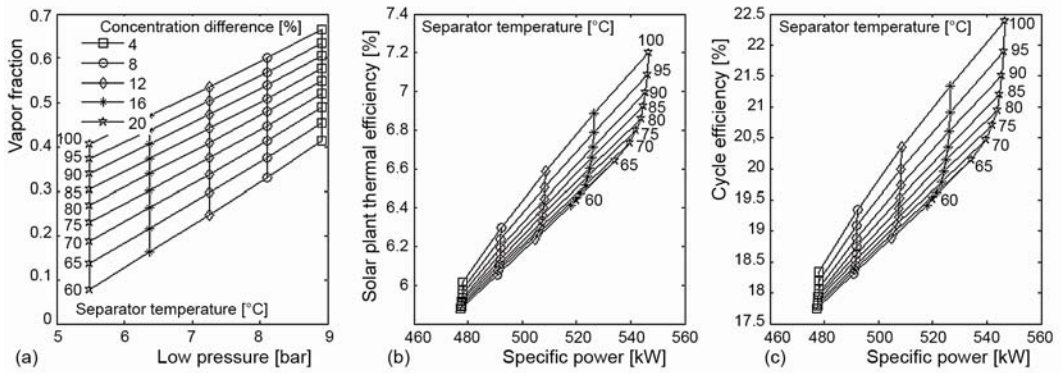

Figure 4. Influence of concentration difference with separator temperature on process conditions, and performance of solar thermal power plant at the turbine inlet concentration of 0.75

17.5–22.5% of cycle efficiency and 480–550 kW of specific work output. The plant efficiency and power output rises with an increment in the separator temperature and concentration difference. That means the plant demands high separator temperature with lower separator inlet concentration. The efficiencies are increasing in increasing order with an increment in separator temperature. But the specific power increases with a decreasing order with the separator temperature. Due to decrease in LP, there is a more expansion in turbine and this causes an increased performance in efficiencies and specific power. Marston [13] reported 32.5% cycle efficiency at a heat source temperature of 500 ºC. The current model results 22.5 % at 500 ºC. The current model shows low efficiency compared to the reported value due to difference in sink value and also the assumption of 75% turbine efficiency against the 90% efficiency of reported results. The literature values are reported at 15 ºC sink temperature, the present values are developed at hot climatic conditions. The increasing trends of cycle efficiency with separator temperature are matched with the Marston [13] and Nag and Gupta [14] results.

Figure 5(a) shows the effect of concentration difference (4-20%) and turbine concentration (0.5-0.8) on vapor fraction and LP. The maximum concentration difference is found as 20% and 0.8 maximum turbine concentration. With the specified variations in concentrations, the resulted LP change is from 1–10 bar and separator vapor fraction varied from

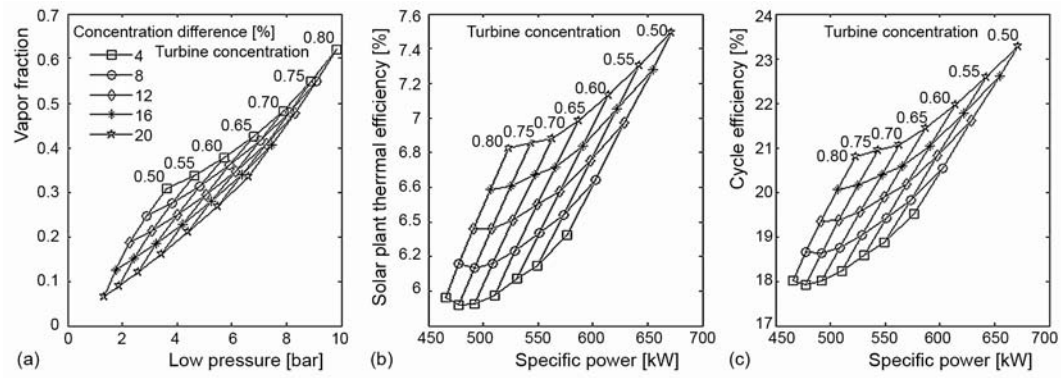

Figure 5. Influence of concentration difference with turbine concentration on process conditions and performance of solar thermal power plant at the turbine inlet condition of 100 bar and 500 °C, and 80 °C of separator temperature

0.1-0.6. The increment in concentration difference at fixed turbine concentration is equal to a drop in separator inlet concentration. Therefore, vapor fraction and LP are increasing with an increase in turbine concentration and separator inlet concentration. If turbine concentration has been increased at a fixed concentration difference, it also results an increase in separator inlet concentration. So, LP rises with turbine inlet concentration and separator concentration. Figures 5(b) and (c) show the trends for efficiencies and power at various concentration differences and turbine concentrations. The efficiencies and power output trends are in opposite compared to the vapor fraction and LP variations. The vapor fraction and LP maximizes at high values of concentrations (separator inlet and turbine inlet) whereas the efficiencies and specific power outputs are maximizing at lower values of these concentrations (high concentration difference). One reason is the turbine expansion decreases with high LP. The second, a low vapor can be separated at low turbine and separator concentrations. With the specified variations in concentrations, the resulted plant, cycle and specific power outputs are 6-7.5%, 18-23%, and 450-675 kW, respectively. The decreasing trends of cycle efficiency with turbine concentration are matched with the literature [13, 14] plots.

Figure 6 shows the effect of turbine inlet pressure (50-100 bar) and collector outlet temperature (250-600 ºC) on (a) solar plant efficiency – specific power and (b) Kalina cycle energy efficiency – specific power. Under the specified limits of operating conditions, the plant results 5.2-6.6% of solar power plant efficiency, 13.5-21% cycle energy efficiency and 250-625 kW of specific power output.

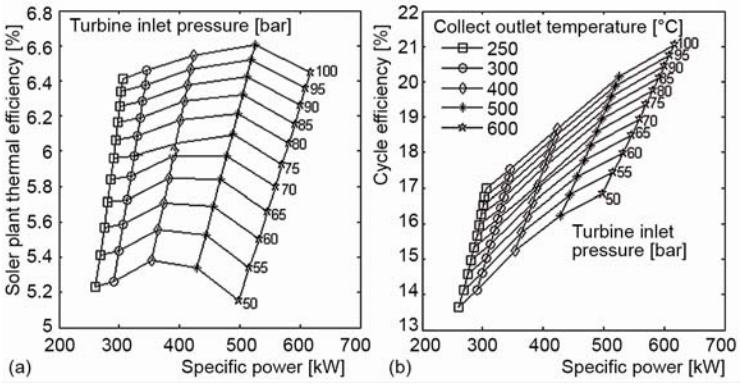

Figure 6. Performance variation of solar thermal power plant with turbine inlet pressure, and temperature at 0.16 concentration difference, 75% turbine concentration, and 80 °C of separator temperature

The maximum suitable heat recovery temperature for Kalina power cycle configuration is 600 ºC at the turbine inlet pressure of 100 bar. At increase in turbine inlet pressure the efficiencies and specific power are increased. A small increment in plant efficiency and a considerable increment in cycle efficiency have been observed from the results. The turbine work increases with a small change in pump work and results an increment in specific work. The results are plotted at constant turbine and separator concentrations. So, LP and IP are constants during changes in the above mentioned parameters. With a rise in collector outlet temperature, cycle efficiency and specific power increases. As per the Carnot law, the cycle thermal efficiency increases with an increase in source temperature. But the plant thermal efficiency increases and then decreases with the source temperature due to involvement of collector efficiency. At high source temperatures, there are more heat losses at the solar concentrating collector. So, up to 75 bar pressure, the plant efficiency maximizing at 400 ºC of supply temperature and at above this pressure, it maximizes at 500 ºC. The cycle efficiency is increasing continuously with an increase in the source temperature.

Figures 7(a), (b), and (c) depict the effect of collector outlet temperature and solar beam radiation on the performance of the solar thermal power plant. The solar direct normal

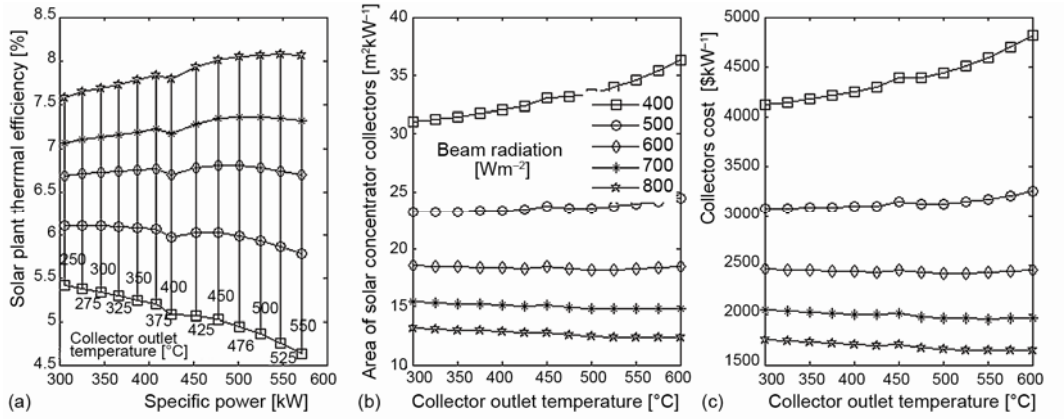

Figure 7. Solar thermal power plant thermo-economic results with solar beam radiation and plant maximum temperature at the turbine inlet condition of 100 bar, 75% concentration, and 80 °C of separator temperature

radiation (DNI) is varied from 400 W/m^2 to 800 W/m^2. The collector outlet temperature is varied from 250 ºC to 550 ºC. With increase in collector temperature, plant thermal efficiency decreases at low beam radiation. At high beam radiation the plant efficiency increases. Specific power increases with increased collector temperature at all the radiations. The maximum plant efficiencies are obtained at the radiations of 400 W/m^2-800 W/m^2 are 5.5%-8% with the source temperature of 250 ºC to 500 ºC. At increased beam radiation, the specific area and specific cost of solar concentrator collectors are reduced as shown in figs. 7(b) and 7(c). The specific area decreased from 36 m^2/kW to 13 m^2/kW whereas the specific cost decreased from $ 5000 to $ 1700.

Table 2 gives the results of the solar thermal power plant at the operating conditions stated in earlier sections. The rating of heat exchangers, power, efficiency and cost details are developed at the unit mass of the working fluid. These specifications are developed at the same conditions defined for tab. 1. Out of the three heat exchangers (HE_1, HE_2, and HE_3), the maximum heat load is observed at the HE_2. The heat load in the boiler is calculated as the summation of heat loads in the economizer, evaporator and super-heater. The cycle efficiency and net work produced by this plant is higher than the steam Rankine cycle at the same operating conditions.

Table 2. Thermodynamic results of high temperature solar thermal power station at hot fluid inlet temperature of 500 °C, turbine inlet condition of 100 bar, 75% concentration, separator temperature of 80 °C and 16% of concentration difference

Description	Result
Vapor fraction in separator, [%]	33.8
Heat load in boiler (ECO + EVA + SH), [kW]	2606
Heat load in HE_1, [kW]	19
Heat load in HE_2, [kW]	830
Heat load in HE_3, [kW]	93
Heat load in absorber, [kW]	1512
Heat load in condenser, [kW]	500
Work output of mixture turbine, [kW]	555
Work input to solution pumps, [kW]	30
Net electricity output, [kW]	525
Kalina cycle energy efficiency, [%]	20.1
Kalina cycle exergy efficiency, [%]	52.8
Solar to electricity efficiency, [%]	6.6
Total area of collectors, [m^2 kW^{-1}]	16
Cost of collectors, [$ kW^{-1}]	2000

Table 3. Comparison of the current work with the literature results at 70 ºC separator temperature [13]

Description	Marston results [13]	Predicted results	Error [%]
Hot water requirement, [kg s^{-1}]	6.62	6.79	2.54
Hot water inlet temperature, [ºC]	500	550	9.09
Hot water outlet temperature, [ºC]	150	150	0
Separator pressure, [bar]	5.5	5.5	0
Low pressure, [bar]	2	2	0
Temperature of working fluid at boiler inlet, [ºC]	39	53	26
Strong solution concentration	0.45	0.44	2.22
Separated liquid concentration	0.34	0.34	0
Vapor separated, [kg s^{-1}]	0.97	0.96	1.03
Ammonia-water mixture before separation, [kg s^{-1}]	2.94	2.82	4.08
Temperature after expansion, [ºC]	118.87	126	5.6
Temperature after pumping, [ºC]	22	25	12
Pump input, [kW]	29.45	24	18.5
Cycle energy efficiency, [%]	32.5	31	4.6

Table 3 compares the present simulated results with the plant readings [13]. The current plant is solved with the working conditions of T_1 = 70 °C, x_{13} = 0.70, P_{13} = 100 bar and $t_{cw,in}$ = 15 °C. Most of the calculated results in this work closely match with the existing results. The strong solution concentration resulted as 0.44. The resulted low pressure is 2 bar. The temperature at the boiler inlet in the existing result is 39 ºC whereas the reported result is 53 ºC.

Conclusions

A solar thermal power plant having Kalina power system has been modelled and analyzed parametrically. The parameters considered for optimization are concentration difference, separator temperature, turbine inlet concentration, turbine inlet pressure, source temperature and solar radiation. The performance of the plant has been studied at the separator temperature of 60-100 ºC, turbine inlet concentration of 0.5-0.8, concentration difference of 4-20%, source temperature of 250-600 ºC and solar beam radiation of 400-800 W/m^2. The maximum cycle energy efficiency obtained from the cycle is about 23.5%, solar plant efficiency is 7.5% and specific work is 675 kW. To understand the performance variations clearly, the changes in vapor fraction and LP are studied with the operational conditions. The maximum efficiencies and specific power are resulted at the minimum values of separator inlet concentration (0.3) and turbine inlet concentration (0.5). To get the maximum solar plant efficiency, an optimum source temperature to be selected suitable to turbine inlet pressure. The minimum collector cost can be obtained with high solar beam radiation and optimized cycle conditions. The thermodynamic model has been validated by comparing with the literature results [13, 14].

Nomenclature

A – area, [m^2]
F – vapor mass fraction in separator
h – specific enthalpy, [kJkg^{-1}]
m – mass, [kgs^{-1}]
q – specific heat, [kJkg^{-1}]
T – temperature, [K]
TTD – terminal temperature difference, [K]
w – specific work output, [kJkg^{-1}]
x – mass fraction of ammonia, [$kgkg^{-1}$] mixture
η – efficiency

Subscripts

b – beam
c – collector
g – global
KC – Kalina cycle
m – mechanical
p – pump
t – turbine
tot – total

References

[1] Ibrahim, O. M., Klein, S. A., Absorption Power Cycles, *Energy, 21* (1996), 4, pp. 21-27
[2] Kalina, A. I., *Direct fired power cycle*, USP 4732005, 1988
[3] Mirolli, M., *et al*., Testing and Operating Experience of the 2 MW Kalina Cycle Geothermal Power Plant in Husavik, Iceland, *Proceedings*, World Renewable Energy Congress VII, Cologne, Germany, 2002
[4] Heppenstall, T., Advanced Gas Turbine Cycles for Power Generation: a Critical Review, *Applied Thermal Engineering, 18* (1998), 9, pp. 837-846
[5] Thorin, E., *et al*., Thermodynamic Properties of Ammonia-Water Mixtures for Power Cycles, *International Journal of Thermophysics, 19* (1998), 2, pp. 501-510
[6] Srinophakun, T., *et al*., Simulation of Power Cycle with Energy Utilization Diagram, *Energy Conversion and Management, 42* (2001), 12, pp. 1437-1456
[7] Dipippo, R., Second Law Assessment of Binary Plants Generating Power from Low-Temperature Geothermal Fluids, *Geothermics*, *33* (2004), 5, pp. 565-586
[8] Borgert, J. A., Velasquez, J. A., Exergoeconomic Optimization of a Kalina Cycle for Power Generation, *Int. J. Exergy*, *1* (2004), 1, pp. 18-28
[9] Mirolli, M., Commercialization of Kalina Cycle for Power Generation and its Potential Impact on CO_2 Emissions, *Proceedings,* International Joint Power Generation Conference*,* New Orleans, La., USA, 2001, pp. 1-7
[10] Minea, V., *Using Geothermal Energy and Industrial Waste Heat for Power Generation*, IEEE, 2007, pp. 543-549
[11] Wall, G., Ishida, C., Exergy Study of the Kalina Cycle, *Analysis and Design of Energy Systems: Analysis of Industrial Processes, AES*, *ASME 10* (1989), 3, pp. 73-77
[12] Wang, J., *et al*., Exergy Analyses and Parametric Optimizations for Different Cogeneration Power Plants in Cement Industry, *Applied Energy*, *86* (2009), 6, pp. 941-948
[13] Marston, C. H., Parametric Analysis of the Kalina Cycle, *ASME Journal of Engineering for Gas Turbines and Power, 112* (1990), 1, pp. 107-116
[14] Nag, P. K., Gupta, A. V. S. S. K. S., Exergy Analysis of the Kalina Cycle, *Applied Thermal Engineering, 18* (1998), 6, pp. 427-439
[15] Shankar Ganesh, N., Srinivas, T., Design and Modeling of Low Temperature Solar Thermal Power Station, *Applied Energy, 91* (2012), 1, pp. 180-186

Paper submitted: June 23, 2012
Paper revised: December 31, 2012
Paper accepted: January 1, 2013